The Molecular Structures of Gaseous Tetrakis(dimethylamino)diboron, $B_2(NMe_2)_4$, and Tetrakis(methoxy)diboron, $B_2(OMe)_4$, as determined by Electron Diffraction

Paul T. Brain,[a] **Anthony J. Downs,***[,a] **Peter Maccallum,**[b] **David W. H. Rankin,**[b] **Heather E. Robertson**[b] **and George A. Forsyth**[b]
[a] *Inorganic Chemistry Laboratory, University of Oxford, South Parks Road, Oxford OX1 3QR, UK*
[b] *Department of Chemistry, University of Edinburgh, West Mains Road, Edinburgh EH9 3JJ, UK*

The structures of gaseous $B_2(NMe_2)_4$ and $B_2(OMe)_4$ have been determined by electron diffraction. The results indicate that the amine adopts the expected fully staggered conformation with D_2 symmetry whilst, surprisingly, the methoxy derivative has not a planar heavy-atom skeleton as thought previously, but a partially staggered conformation. Salient structural parameters (r_a) are (*i*) for $B_2(NMe_2)_4$, r(B–B) 176.2(1.1) and r(B–N) 140.8(3) pm; NBBN 90.0(1.1), NBN 124.0(5) and BBNC 19.7(1.1)°; and (*ii*) for $B_2(OMe)_4$, r(B–B) 172.0(6) and r(B–O) 136.9(3) pm; OBBO 49.5(1.2), OBO 119.9(4) and BBOC 12.1(2.7) and 21.9(1.9)° (clockwise and anticlockwise out of the BBO plane).

Many compounds of the general formula B_2X_4 (X = halogen atom, NR_2 or OR) have been synthesised.[1] In comparison to the wealth of structural information which has been accumulated for monoboron compounds BX_3,[2–7] however, definitive structural characterisation has been realised for comparatively few diboron compounds.[8–13]

Tetrakis(dimethylamino)diboron, $B_2(NMe_2)_4$, and tetrakis(methoxy)diboron, $B_2(OMe)_4$, have proved to be very useful precursors to other diboron compounds.[14] Amongst the most thermally stable of diboron compounds, they readily undergo ligand-exchange reactions,[14] and numerous tetrakis(amino)- and tetrakis(alkoxy)-diboron compounds have thus been prepared from $B_2(NMe_2)_4$. Although certain of these products have been characterised structurally by X-ray crystallography,[11–13] however, no structural studies of the parent compounds $B_2(NMe_2)_4$ and $B_2(OMe)_4$ have been ventured previously.

To rectify this situation, and as part of a wider study of molecules containing boron–boron bonds,[15,16] the structures of gaseous $B_2(NMe_2)_4$ and $B_2(OMe)_4$ have been investigated by electron diffraction. The configurations and dimensions are compared with those of other B_2X_4 and analogous BX_3 compounds and discussed with regard to possible π back-bonding and steric effects.

Experimental

Synthesis.—Tetrakis(dimethylamino)diboron and tetrakis(methoxy)diboron were prepared by the methods of Brotherton *et al.*[17,18] The purity of each of the compounds was checked by reference (*i*) to the IR spectra of the vapour and/or a solid film at 77 K and (*ii*) to the ^1H, ^{11}B and ^{13}C NMR spectra of $CDCl_3$ solutions.[19–21]

Electron-diffraction Measurements.—Electron-scattering measurements were recorded on Kodak Electron Image plates using the Edinburgh gas-diffraction apparatus operating at *ca.* 45 kV (electron wavelength *ca.* 5.7 pm).[22] Nozzle-to-plate distances were *ca.* 94 and 260 mm for $B_2(NMe_2)_4$ and *ca.* 128 and 286 mm for $B_2(OMe)_4$; three plates were recorded at each distance. With $B_2(NMe_2)_4$ the sample and nozzle were maintained at 337 and 358 K, respectively, whereas with $B_2(OMe)_4$ the sample and nozzle were both maintained at 288 K throughout the exposure periods. The precise nozzle-to-plate distances and electron wavelengths were determined by reference to the scattering patterns for benzene vapour recorded immediately before and after each set of sample plates. Details are given in Table 1, together with the weighting functions used to set up the off-diagonal weight matrices, the correlation parameters and the final scale factors.

Details of the electron-scattering patterns were converted into digital form using a computer-controlled Joyce-Loebl MDM6 microdensitometer with a scanning program described elsewhere.[23] The programs used for data reduction[23] and least-squares refinement[24] have been described previously, the complex scattering factors being those listed by Fink and Ross.[25] The scattering patterns of benzene were analysed in exactly the same way as those of the diboron compounds so as to minimise systematic errors in the wavelengths and camera distances.

Results

Structural Analysis: Molecular Models.—The molecular models used to generate the atomic coordinates of $B_2(NMe_2)_4$ and $B_2(OMe)_4$ are described by the molecular parameters listed in Tables 2 and 3, respectively.

$B_2(NMe_2)_4$. The model was based largely on the structure established for $B(NMe_2)_3$.[3] The B–N, N–C and C–H bond distances were assumed to be constant throughout the molecule. The BBN_2 and BNC_2 units were kept planar with BNC_2 units allowed to twist out of the BBN_2 plane and related to each other by C_2 symmetry about the B–B bond. Each of the methyl groups was assumed to have local C_{3v} symmetry and the NMe_2 groups to maintain C_2 symmetry about the B–N bond. Other independent parameters were the BNC and NCH angles and the BBNC and BNCH torsion angles. Thus, relative to the $B(NMe_2)_3$ structure,[3] the NBN angle was allowed to vary from 120°, and the two BNC angles of each NMe_2 group were also allowed to vary to admit the possibility of some asymmetry. The B–B distance and the NBBN torsion angle were included as independent parameters although it seemed reasonable to assume, on the evidence of the structures adopted by the diboron tetrahalides,[8–10] that the N_2BBN_2 skeleton of the

Table 1 Nozzle-to-plate distances, weighting functions, correlation parameters, scale factors and electron wavelengths

Molecule	Nozzle-to-plate distance/mm	Δs/nm^{-1}	s_{min}/nm^{-1}	sw_1/nm^{-1}	sw_2/nm^{-1}	s_{max}/nm^{-1}	Correlation, p/h	Scale factor, k^a	Electron wavelength^b/pm
$B_2(NMe_2)_4$	259.0	2	20	40	144	164	0.4713	0.702(3)	5.674
	94.4	4	80	60	404	328	−0.0347	0.592(11)	5.670
$B_2(OMe)_4$	285.9	2	20	40	122	144	0.4638	0.794(4)	5.671
	128.2	4	80	100	276	324	0.2842	0.842(17)	5.672

[a] Figures in parentheses are the e.s.d.s of the last digits. [b] Determined by reference to the scattering pattern of benzene vapour.

Table 2 Molecular parameters for $B_2(NMe_2)_4$[a]

Parameter		Distance/pm or angle/°	Amplitude/pm
(*a*) Independent			
r_1	r(B–B)	176.2(1.1)	5.0^b
r_2	r(B–N)	140.8(3)	3.6^b
r_3	r(N–C)	147.2(1)	3.6^b
r_4	r(C–H)	111.7(2)	7.6(2)
p_1	NBN	124.0(5)	
p_2	τ(NBBN)	90.0^b	
p_3	CNC	109.2(6)	
p_4	CNC difference	0.0^b	
p_5	τ(BBNC)	19.7(1.1)	
p_6	NCH	110.2(5)	
p_7	τ(BNCH)	0.0^b	
(*b*) Dependent^c			
r_5	r(H···H)	181.6(7)	12.0^b
r_6	r(H···N)	213.3(6)	10.1(5)
r_7	r(C···C)	240.0(7)	7.3(1.1)
r_8	r(C···B)	255.9(3)	7.7(8)
r_9	r(N···N)	248.6(7)	5.6(1.2)
r_{10}	r(N···B)	272.3(8)	11.3(1.5)
r_{11}	r[C(1)···N(2)]	383.7(6)	8.6^b
r_{12}	r[C(1)···B(2)]	314.2(8)	12.1^b
r_{13}	r[C(2)···N(2)]	307.4(8)	13.0^b
r_{14}	r[C(2)···B(2)]	411.2(9)	8.0^b
r_{15}	r[N(1)···N(3)]	354.9(7)	24.3^b
r_{16}	r[C(2)···C(4)]	303.9(1.8)	13.5^b
r_{17}	r[C(1)···C(5)]	354.5(2.5)	32.1^b
r_{18}	r[C(1)···N(3)]	364.2(1.0)	14.2^b
r_{19}	r[C(1)···N(4)]	390.8(1.5)	18.6^b

[a] Figures in parentheses are the e.s.d.s of the last digits. [b] Refined then fixed. See text. [c] Other non-bonded distances were included in the refinement (over 140 in total) but are not listed here.

Table 3 Molecular parameters for $B_2(OMe)_4$[a]

Parameter		Distance/pm or angle/°	Amplitude/pm
(*a*) Independent			
r_1	r(B–B)	172.0(6)	7.2(1.2)
r_2	r(B–O)	136.9(3)	4.6(2)
r_3	r(O–C)	143.2(2)	4.6 (tied to u_2)
r_4	r(C–H)	109.5(3)	8.9(3)
p_1	OBO	119.9(4)	
p_2	τ(OBBO)	49.5(1.2)	
p_3	BOC	120.8(3)	
p_4	τ(BBOC)	21.9(1.9)	
p_5	OCH	110.0(5)	
p_6	τ(BOCH)	18.6(1.4)	
p_7	BBOC difference	146.1(2.7)	
(*b*) Dependent^c			
r_5	r[O(1)···O(2)]	237.0(3)	6.5^b
r_6	r[O(1)···B(2)]	268.2(3)	7.3^b
r_7	r[C(1)···B(1)]	243.6(4)	11.0^b
r_8	r(H···O)	207.9(6)	11.4(5)
r_9	r(H···H)	178.2(9)	12.0 (tied to u_8)
r_{10}	r[O(1)···C(2)]	279.5(5)	6.4^b
r_{11}	r[O(2)···C(1)]	365.9(5)	6.7^b
r_{12}	r[C(2)···C(1)]	420.1(7)	22.0^b
r_{13}	r[B(1)···C(3)]	301.9(1.1)	13.1^b
r_{14}	r[B(1)···C(4)]	401.2(6)	17.8^b
r_{15}	r(H···B)	253.6(1.1)	15.0^b
r_{16}	r(H···B)	303.4(1.3)	15.0^b
r_{17}	r(H···B)	324.7(8)	15.0^b
r_{18}	r[O(1)···O(4)]	324.8(8)	18.1^b
r_{19}	r[O(1)···O(3)]	376.7(9)	25.8^b
r_{20}	r[C(1)···C(4)]	325.4(1.5)	18.1^b
r_{21}	r[C(1)···O(3)]	403.6(1.8)	17.8^b
r_{22}	r[H′···O(1)]	238.5(1.8)	20.0^b

[a] Figures in parentheses are the e.s.d.s of the last digits. [b] Refined then fixed. See text. [c] Other non-bonded distances were included in the refinement (99 in total). Those not shown had their amplitudes of vibration set to 20.0 pm.

compound would adopt a staggered conformation with D_{2d} symmetry.

The symmetry relating the two $B(NMe_2)_2$ fragments together was also considered. This takes the form of either (*i*) a reflection through a plane or (*ii*) a rotation about an axis perpendicular to the B–B bond, followed by a torsional motion about the B–B bond. In the fully staggered case, with an NBBN dihedral angle of 90°, these two conformations correspond to overall symmetries of S_4 or D_2, respectively.

$B_2(OMe)_4$. The model was essentially similar to that employed for $B_2(NMe_2)_4$. The major difference (apart from the absence of four methyl groups) was that the two methyl groups of each $B(OMe)_2$ moiety were allowed to rotate independently about the B–O bonds, *i.e.* an angle was included which permitted the Me groups to move from positions complying with C_2 symmetry about the B–B bond.

Refinement of the Structure of $B_2(NMe_2)_4$.—The radial distribution curve for $B_2(NMe_2)_4$ [Fig. 1(*a*)] shows two peaks below 200 pm near 110 and 140 pm corresponding to scattering from C–H, B–N and N–C bonded atom pairs, the last two contributing to the peak near 140 pm. Apart from the distinct peak at *ca.* 250 pm, which is due to scattering from C···C, C···B, N···N and N···B non-bonded pairs, the radial distribution curve at $r > 200$ pm consists of a broad feature involving many maxima attributable to the large number of distinct non-bonded distances in the molecule.

The radial distribution curve for $B_2(NMe_2)_4$ could be accounted for most satisfactorily by refinement of the model adopting D_2 symmetry. This implies a fully staggered conformation [NBBN dihedral angle = 90.0(1.1)°] with no significant asymmetry of the NC_2 units [difference in CNC angle = 0.2(4)°]. The values of these parameters were subsequently fixed at 90 and 0°, respectively, in the final stages of the refinement calculations. The BNCH torsion angle did not refine well [5.0(7.0)°]; the best refinements were found in a range extending ± 10° from this value and so the angle was fixed at 0°.

With the above parameters fixed, the other independent distances and angles all refined well. The largest uncertainty affecting the bond lengths is associated with r(B–B) [176.2(1.1) pm]. This arises because the B–B atom pair has a relatively low scattering intensity. The largest estimated standard deviation

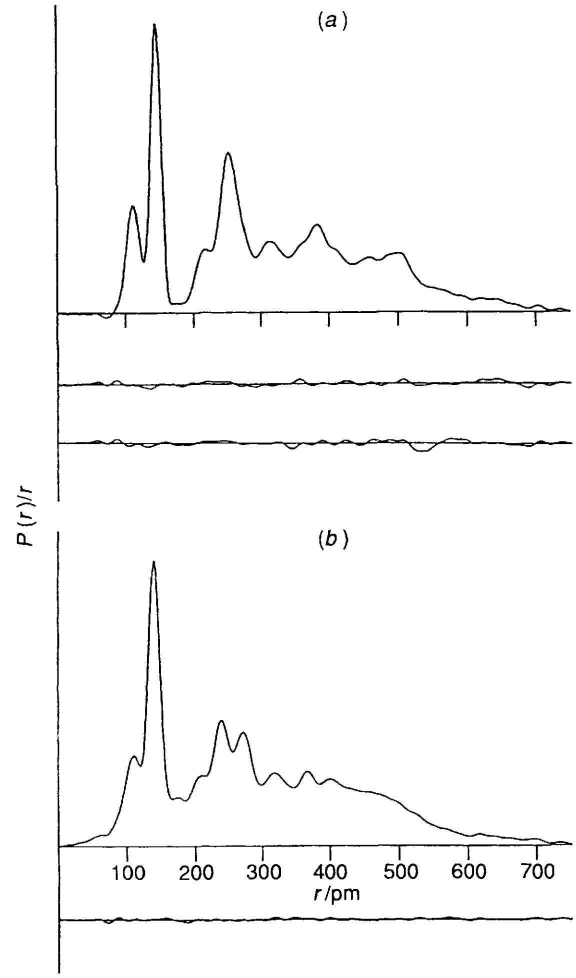

Fig. 1 Observed and final weighted difference radial distribution curves (*a*) for $B_2(NMe_2)_4$ and (*b*) for $B_2(OMe)_4$. For $B_2(NMe_2)_4$ the upper and lower difference curves correspond to the D_2 and S_4 model structures respectively. Before Fourier inversion the data were multiplied by $s\cdot\exp[(-0.000\,02s^2)/(Z_x - f_x)(Z_c - f_c)]$ (where X = N or O)

(e.s.d.) affecting the angles is associated with the BBNC torsion angle [19.7(1.1)°]; this reflects the uncertainties in the distances and angles defining the parameter.

Refinement of the amplitudes of vibration produced mainly stable values with acceptable margins of error. However, it was found necessary to fix the B–B value, which had a tendency to increase, and the B–N and N–C values, which decreased beyond the reasonable range. The B–N and N–C atom pairs subscribed to a common peak in the radial distribution curve and thus induced false refinements of their u values. By performing a series of refinements in which these amplitudes of vibration were fixed at various values, it was possible to estimate the extent to which fixing them affected the refined B–B, B–N and N–C distances. It was concluded that the exclusion of these amplitudes of vibration from the final refinement leads probably to an underestimate of the e.s.d.s for these distances by a factor of between 2.0 and 2.5.

The S_4 model refined less well (R_G = 0.113) than the D_2 model (R_G = 0.095). This difference seems to be significant, although the possibility that the vapour consists of a mixture of the two conformers cannot be ruled out.

The success of the final refinement may be assessed on the basis of the difference between the experimental and calculated radial distribution curves [Fig. 1(*a*)]. Fig. 2(*a*) offers a similar comparison between the experimental and calculated molecular scattering intensities. The structural details and vibrational amplitudes of the optimum (D_2) refinement are listed in Table 2 and Fig. 3(*a*) affords a perspective view of the molecule. Salient features of the least-squares correlation matrix appear in Table 4(*a*).

Table 4 Portions of the least-squares correlation matrices (*a*) for $B_2(NMe_2)_4$ and (*b*) for $B_2(OMe)_4$ showing off-diagonal elements greater than 50%

(*a*)

r_1	r_3	u_7	u_8	u_9	u_{10}	k_2*	
	−60					−68	r_2
						61	r_3
78							p_1
				69			p_3
		51					p_6
			72		51		u_7
					70		u_8

(*b*)

r_1	r_2	r_3	p_4	p_7	u_2	k_2*	
	−72	64			−64		r_1
		−88			79		r_2
					−79		r_3
78	−73	64			−57		p_1
			−70	71			p_2
				−75			p_4
						52	u_2

* Scale factor.

Refinement of the Structure of $B_2(OMe)_4$.—The radial distribution curve for $B_2(OMe)_4$ [Fig. 1(*b*)] shows three peaks in the region associated with bonded distances, with distinct peaks for the C–H and B–B distances at *ca.* 110 and 170 pm, respectively, but with those for B–O and O–C overlapping at *ca.* 140 pm. As with $B_2(NMe_2)_4$, the radial distribution curve at $r > 200$ pm consists of a broad feature with a number of maxima, the most intense of which occur at *ca.* 240 pm, corresponding to scattering from O • • • O and C • • • B non-bonded pairs, and *ca.* 270 pm, corresponding to scattering from O • • • B and O • • • C non-bonded pairs.

All eleven of the independent geometrical parameters used to define the molecular model of $B_2(OMe)_4$ yielded to simultaneous refinement. An initial refinement led to a structure with an R_G factor of 0.22. This was recognised as false, however, through its requirement of an unreasonable degree of C(1)–C(3) crowding, and it was accordingly rejected.

The amplitudes of vibration for the bonded distances all refined realistically when treated individually. However, since the B–O and C–O bond distances lie under the same peak in the radial distribution curve, it was necessary to constrain their amplitudes of vibration to be equal.

The geometrical parameters obtained in the final refinement, for which R_G = 0.070, are listed in Table 3, and details of the least-squares correlation matrix are given in Table 4(*b*). Fig. 3(*b*) offers a perspective view of the molecule and Fig. 2(*b*) illustrates the observed and final difference curves for the molecular scattering intensities.

The relative complexity and low symmetry of the molecules $B_2(NMe_2)_4$ and $B_2(OMe)_4$, allied to the lack of any rigorously based vibrational assignments, ruled out the possibility of applying any shrinkage corrections. However, there is no reason to suppose that such corrections would alter significantly the principal results of our calculations.

Discussion

The structure of neither of the gaseous molecules $B_2(NMe_2)_4$ and $B_2(OMe)_4$ has been reported previously. In the case of $B_2(NMe_2)_4$, the vibrational spectra of the liquid and the photoelectron spectrum of the vapour have been reinterpreted in terms of a fully staggered conformation.[20] The only

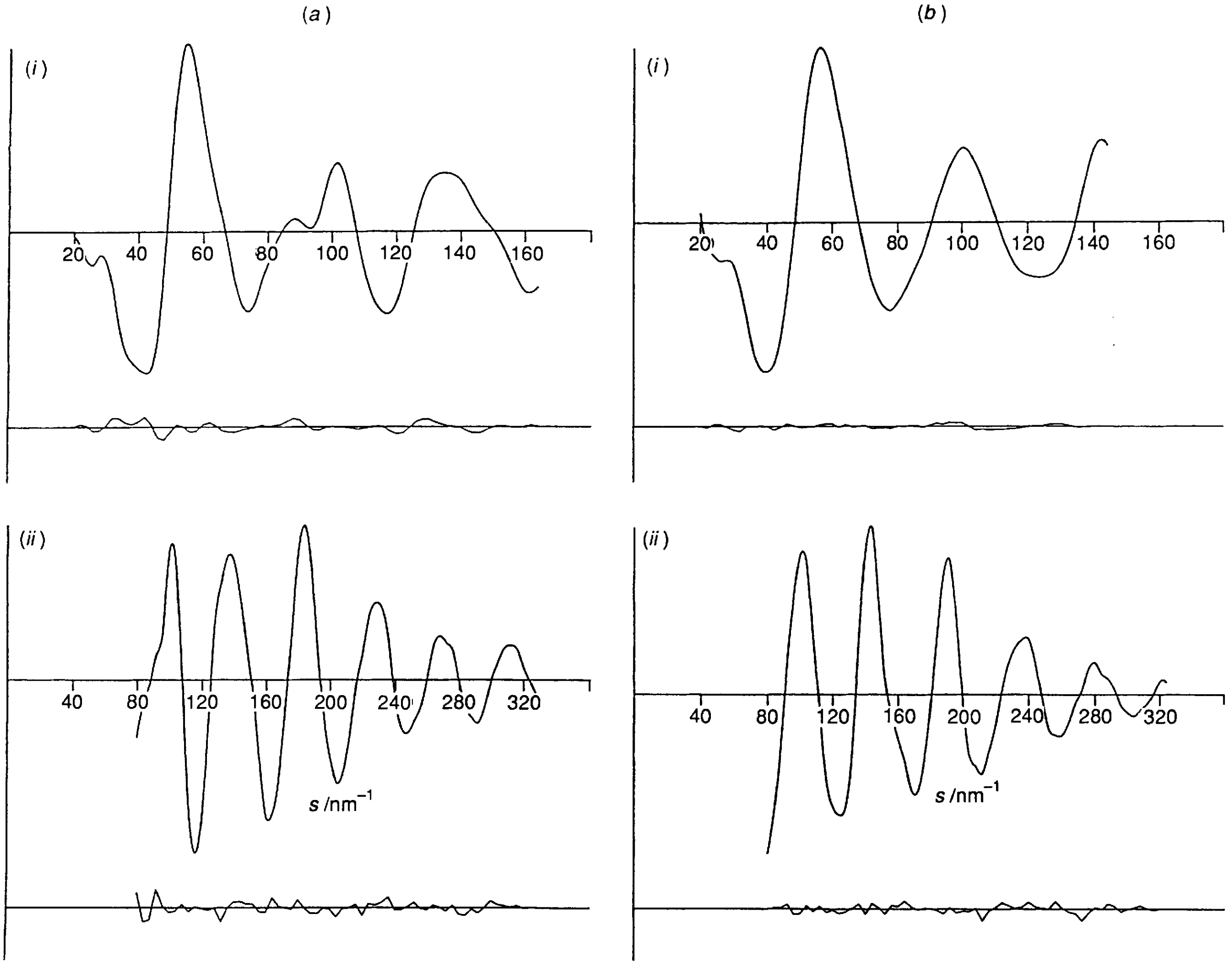

Fig. 2 Observed and final weighted difference molecular scattering intensity curves (*a*) for $B_2(NMe_2)_4$ and (*b*) for $B_2(OMe)_4$. Nozzle-to-plate distances were (*a*) 259.0 (*i*) and 94.4 mm (*ii*) and (*b*) 285.9 (*i*) and 128.2 mm (*ii*)

vibrational results available for $B_2(OMe)_4$ seemingly suggest a molecule with a planar heavy-atom skeleton conforming to C_{2h} symmetry.[19] The results that we have deduced from the electron-diffraction patterns are thus quite new for both $B_2(NMe_2)_4$ and $B_2(OMe)_4$. Our analysis confirms that gaseous $B_2(NMe_2)_4$ adopts a fully staggered conformation with D_2 symmetry. Contrary to the interpretation of the vibrational properties,[19] however, gaseous $B_2(OMe)_4$ is found to have a partially staggered conformation with a torsion angle of *ca.* 50°. Although it is possible that some modification of the structure occurs with the transition from the gas to the liquid phase, it is our opinion that the earlier vibrational measurements on $B_2(OMe)_4$ have been incorrectly interpreted [as were the corresponding measurements on $B_2(NMe_2)_4$ in the same study].[19,20]

Collation of the dimensions of $B_2(NMe_2)_4$ and $B_2(OMe)_4$ with those of related mono- and di-boron compounds (see Tables 5 and 6) brings to light a number of noteworthy features, which are considered below.

The B–B bond length in $B_2(NMe_2)_4$, at 176.2(1.1) pm, is the longest known for B_2X_4-type molecules; in gaseous B_2F_4, B_2Cl_4 and B_2Br_4 the corresponding distance is 172.0(4), 170.2(6.9) and 168.9(1.6) pm, respectively.[8–10] It would appear that, even though a fully staggered conformation is adopted, considerably more steric repulsion occurs between the NR_2 units in $B_2(NMe_2)_4$ than in the other tetrakis(amino)diboron compounds whose structures have been determined to date (Table 5). Such a finding is to be expected in the light of the NBN angle; an increase of nearly 20° in this angle in the switch from compounds **1** and **2**[11,13] to $B_2(NMe_2)_4$ must imply a marked increase in the steric repulsion across the B–B bond, which is thereby attenuated significantly, in $B_2(NMe_2)_4$.

The B–N bond length in $B_2(NMe_2)_4$ is typical of an aminoborane, as testified by the data in Table 5. It is, however, more than 2 pm shorter than the corresponding distance in $B(NMe_2)_3$, suggesting an increased π contribution to the bonding. This can be seen as a result of the smaller BNC torsion angle [*ca.* 20° in $B_2(NMe_2)_4$ compared with *ca.* 33° in $B(NMe_2)_3$], a change leading to greater π-type overlap of the boron and nitrogen 2p orbitals. The magnitude of the BNC torsion angle is determined by the NBN angle which is greater in $B_2(NMe_2)_4$ than in $B(NMe_2)_3$ because of the reduced steric interactions of the NMe_2 units across the B–B bond. Such arguments involving π-type bonding are consistent but, at best, speculative, and the shortening of the B–N bond may simply be a *direct* result of the reduced non-bonded steric interactions.

The B–B bond length in $B_2(OMe)_4$, at 172.0(6) pm, is the same as that found in B_2F_4 [172.0(4) pm].[8] Steric factors in B_2F_4 are partially offset by B–F π-type back bonding throughout the molecule giving a planar molecule as the form lowest in energy but with the longest B–B bond of the diboron tetrahalides.[8–10] With $B_2(OMe)_4$, steric factors must be presumed to cause a twisting about the B–B bond but at the expense of the through-molecule π bonding.

The B–O bond distance in $B_2(OMe)_4$ is not unusual for compounds of this type (see Table 6), being typical of boron–oxygen bonds thought to derive some contribution from π back bonding.[6] It is, interestingly, some 4.5 pm longer than the

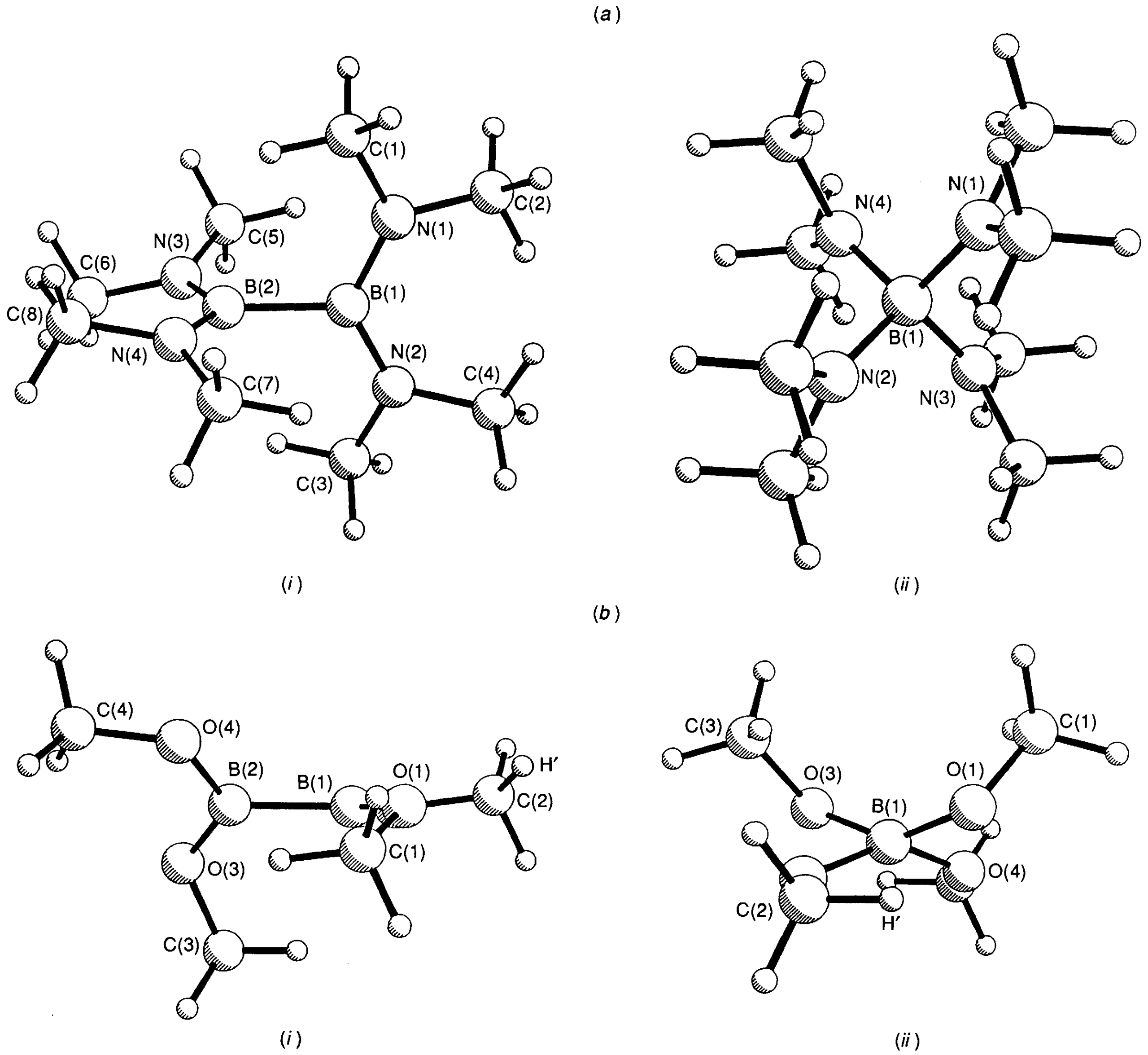

Fig. 3 Optimum structures of (*a*) $B_2(NMe_2)_4$ (D_2 symmetry) and (*b*) $B_2(OMe)_4$: (*i*) perspective view and (*ii*) view along the B–B bond

Table 5 Structural parameters (distances in pm, angles in °) of some aminoboranes

Compound	Technique[a]	*r*(B–B)	*r*(B–N)	τ(NBBN)	NBN	τ(BBNC)	Ref.
$B_2(NMe_2)_4$	ED	176.2(1.1)	140.8(3)	90[b]	124.0(5)	19.7(1.1)	This work
1	XRD	169.3(9)	141.3(8)	*ca.* 60	106.6(6)	—	11
2	XRD	172.1(1.2)	139.3(7)	80.7(8)	109.0(5)	—	13
$B(NMe_2)_3$	ED	—	143.1(1.2)	—	120[c]	32.8(2.6)	3
$B(NHMe)_3$	ED	—	143.2(2)	—	120[c]	13.3(2.1)	4
$BMe(NHMe)_2$	ED	—	141.8(2)	—	120.4(3)	16.9(2.3)	4
$BMe_2(NHMe)$	ED	—	139.7(2)	—	—	7.9(6.2)	4
$BCl_2(NMe_2)$	ED	—	137.9(6)	—	—	0.0(3.0)	5

[a] ED = Electron diffraction (vapour), XRD = X-ray diffraction (crystal). [b] Refined then fixed. [c] Fixed.

Table 6 Structural parameters (distances in pm, angles in °) of some alkoxyboranes

Compound	Technique	*r*(B–B)	*r*(B–O)	τ(OBBO)	OBO	τ(BBOC)	Ref.
$B_2(OMe)_4$	ED	172.0(6)	136.9(3)	49.5(1.2)	119.9(4)	21.9(1.9)	This work
3	XRD	171.1(6)	132.4(4)[a]	0	111.1(2)	—	12
$B(OMe)_3$	ED	—	136.8(2)	—	120[b]	0[b]	6
$BMe(OMe)_2$	ED	—	137.5(4)	—	117.1(1.1)	11.9(7.6)	6
$BMe_2(OMe)$	ED	—	136.1(2)	—	—	14.1(3.8)	6

[a] Average value. [b] Refined then fixed.

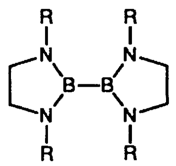

1 R = Me
2 R = C_6H_{11}

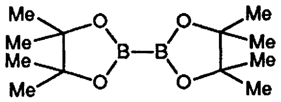

3

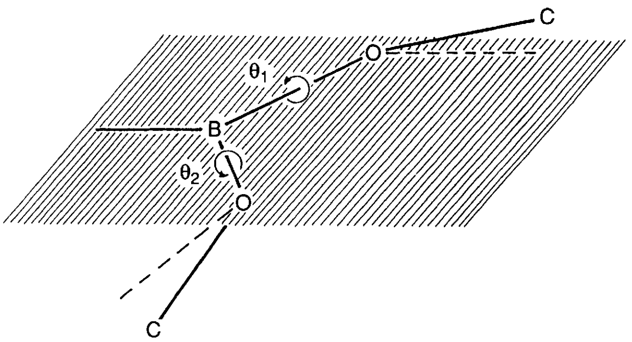

Fig. 4 The $B(OMe)_2$ moiety of $B_2(OMe)_4$ showing the uniquely asymmetric disposition of the methoxy groups. $\theta_1 = 21.9(1.9)$ and $\theta_2 = 12.1(2.7)°$; the dashed lines denote the position of the O–C bond for $\theta_1 = \theta_2 = 0°$

B–O bond length in compound **3**,[12] which represents the only other tetrakis(alkoxy)diboron compound to be characterised structurally up to the present time. Unlike $B_2(OMe)_4$, compound **3** possesses a planar O_2BBO_2 skeleton so that the degree of through-molecule π bonding is optimised. The short B–O distance is thought to manifest this effect, but of the concomitant shortening of the B–B distance there is no sign. It follows that the effects of π bonding must be offset by substantial steric repulsion across the B–B bond. Moreover, the conformation adopted by **3** may well be dictated, on balance, by crystal-packing forces. Free of such forces in the gas phase, the compound may favour a staggered conformation similar to that found for $B_2(OMe)_4$, probably with a shorter B–B bond. A well known precedent is provided by the B_2Cl_4 molecule which is planar in the solid state [r(B–B) = 175 pm][26] and fully staggered in the gas phase [r(B–B) = 170.2 pm].[9]

The methyl groups in $B_2(OMe)_4$ are twisted out of the BBO plane to reduce steric crowding. This option is not available to $B(OMe)_3$ but is observed for other monoboron alkoxy compounds.[6] The angles of twist about the B–O bond are 12.1(2.7)° clockwise, for the inward pointing OMe group, and 21.9(1.9)° anticlockwise, for the outward pointing OMe group, out of the BBO plane for each $B(OR)_2$ moiety (see Fig. 4). To the best of our knowledge, this asymmetry is unique to $B_2(OMe)_4$.

Acknowledgements

We thank the SERC for the award of a research studentship (to P. T. B.), for financial support of the Edinburgh electron-diffraction service (including the funding of H. E. R.'s research assistantship) and for provision of microdensitometer facilities.

References

1 A. G. Massey, *Adv. Inorg. Chem. Radiochem.*, 1983, **26**, 16.
2 *Gmelin Handbook of Inorganic Chemistry*, Springer, Berlin, 1978, Teil 19, pp. 49, 118, 191 and 220.
3 A. H. Clark and G. A. Anderson, *Chem. Commun.*, 1969, 1082.
4 A. Almenningen, G. Gundersen, M. Mangerud and R. Seip, *Acta Chem. Scand., Ser. A*, 1981, **35**, 341.
5 F. B. Clippard, jun., and L. S. Bartell, *Inorg. Chem.*, 1970, **9**, 2439.
6 G. Gundersen, T. Jonvik and R. Seip, *Acta Chem. Scand., Ser. A*, 1981, **35**, 325.
7 K. Brendhaugen, E. W. Nilssen and H. M. Seip, *Acta Chem. Scand.*, 1973, **27**, 2965; S. Lindøy, H. M. Seip and R. Seip, *Acta Chem. Scand., Ser. A*, 1976, **30**, 54; R. Johansen, E. W. Nilssen, H. M. Seip and W. Siebert, *Acta Chem. Scand.*, 1973, **27**, 3015.
8 D. D. Danielson, J. V. Patton and K. Hedberg, *J. Am. Chem. Soc.*, 1977, **99**, 6484.
9 R. R. Ryan and K. Hedberg, *J. Chem. Phys.*, 1969, **50**, 4986.
10 D. D. Danielson and K. Hedberg, *J. Am. Chem. Soc.*, 1979, **101**, 3199.
11 H. Fusstetter, J. C. Huffman, H. Nöth and R. Schaeffer, *Z. Naturforsch., Teil B*, 1976, **31**, 1441.
12 H. Nöth, *Z. Naturforsch., Teil B*, 1984, **39**, 1463.
13 G. Ferguson, M. Parvez, R. P. Brint, D. C. M. Power, T. R. Spalding and D. R. Lloyd, *J. Chem. Soc., Dalton Trans.*, 1986, 2283.
14 *Gmelin Handbook of Inorganic Chemistry*, Springer, Berlin, 1975, Teil 4, pp. 268–276, 1977, Teil 16, pp. 26–30.
15 P. T. Brain, A. J. Downs, M. Fanfarillo, M. J. Goode, A. G. Massey, D. W. H. Rankin and H. E. Robertson, *J. Mol. Struct.*, 1989, **192**, 163.
16 P. T. Brain and A. J. Downs, unpublished work.
17 R. J. Brotherton, A. L. McCloskey, L. L. Petterson and H. Steinberg, *J. Am. Chem. Soc.*, 1960, **82**, 6242.
18 R. J. Brotherton, A. L. McCloskey, J. L. Boone and H. M. Manasevit, *J. Am. Chem. Soc.*, 1960, **82**, 6245.
19 H. J. Becher, W. Sawodny, H. Nöth and W. Meister, *Z. Anorg. Allg. Chem.*, 1962, **314**, 226.
20 G. Davidson and S. Phillips, *J. Chem. Soc., Dalton Trans.*, 1981, 306.
21 H. Nöth and B. Wrackmeyer, *NMR Basic Principles and Progress*, No. 14, Springer, Berlin, 1978.
22 C. M. Huntley, G. S. Laurenson and D. W. H. Rankin, *J. Chem. Soc., Dalton Trans.*, 1980, 954.
23 S. Cradock, J. Koprowski and D. W. H. Rankin, *J. Mol. Struct.*, 1981, **77**, 113.
24 A. S. F. Boyd, G. S. Laurenson and D. W. H. Rankin, *J. Mol. Struct.*, 1981, **71**, 217.
25 M. Fink and A. Ross, *International Tables for Crystallography*, International Union of Crystallography, in the press.
26 M. Atoji, P. J. Wheatley and W. N. Lipscomb, *J. Chem. Phys.*, 1957, **27**, 196.

Received 10*th September* 1990; *Paper* 0/04116E